

Imaging Bio-electro-mechanics with Scanning Probe Microscopy:

Unveiling Nature's Nanoscale Form and Function

S. Jesse,¹ A.P. Baddorf,¹ B.J. Rodriguez,² A. Gruverman,² and S.V. Kalinin¹

¹Condensed Matter Sciences Division, Oak Ridge National Laboratory, Oak Ridge, TN 37831

²Department of Materials Science and Engineering, North Carolina State University, Raleigh, NC 27695

ABSTRACT

Since the discovery in the late eighteenth century of electrically induced mechanical response in muscle tissue, coupling between electrical and mechanical phenomena has been shown to be a ubiquitous feature of biological systems. Here, we measure the local electromechanical properties of biological samples using piezoresponse force microscopy (PFM). This technique is combined with atomic force acoustic microscopy (AFAM) for simultaneous mapping the topography, structure, and electro-mechanical behavior of biological systems down to nanometer scales. We demonstrate the capability of these scanning probe microscopy (SPM) techniques to visualize as of yet unseen spatial variations in the composition and structure of calcified tissues, such as antlers, with 5 nm spatial resolution as well as local mechanical properties variation in a butterfly wing.

Keywords: scanning probe microscopy, piezoresponse force microscopy, molecular imaging

1 INTRODUCTION

Strong coupling between electrical stimulus and mechanical response in biological systems has been known at least since Galvani first reported voltage induced muscle contraction over 200 years ago. Intrinsic electro-mechanical coupling in biological materials is more the rule than the exception and is evident across a wide range of length scales from that of tissues, to cells, to individual biomolecules. One of the most common manifestations of electromechanical coupling is the piezoelectric effect, where applied electric fields induce changes in the atomic spacing and thus changes in the overall shape of noncentrosymmetrical crystal structures including those found in biopolymers, such as cellulose, collagen, and keratin. Piezoelectric behavior is therefore apparent in a variety of biological systems including bones,^{1,2,3,4} teeth,⁵ wood,^{6,7} and seashells.⁸ PFM is a technique that measures highly localized electromechanical coupling and utilizes variations in the intrinsic piezoelectric orientation to generate high resolution maps of topography, structural properties and molecular orientation.

Despite the lack of fundamental evidence, piezoresponse in bio-systems was argued to serve very important biological functions. Because piezoelectric behavior can act as a transducer converting strain to

electric charge, it has been postulated that the electromechanical coupling evident in organisms may be a mechanism in directing local tissue development^{9,10} and may also be in part responsible for cell differentiation. Understanding the relationship between physiologically generated electric fields and mechanical properties on the molecular, cellular and tissue levels has become an important motivation in studying piezoelectricity in biological systems, and a number of approaches for controlling bone healing and regeneration using electric stimulation and piezoelectric implants has been proposed. Here, we demonstrate local imaging of electromechanical coupling in biological systems on the nanometer scale using PFM, opening a new pathway for the investigation of developmental phenomenon.

2 EXPERIMENTAL TECHNIQUES

The PFM principle is based on the detection of local electromechanical coupling - an electrical bias is applied to the tip, and the resulting surface deformation is recorded over an array of positions on the sample surface. PFM is operated in contact mode and a conductive PFM tip is biased, relative to the substrate, with a signal composed of a single frequency sinusoidal component and a DC offset (Fig. 1(a)). A strong and highly localized oscillating electric field is consequently generated at the tip/surface interface and any piezoelectric material will respond and oscillate at the driving frequency with a particular phase offset and in a direction dependent upon local crystallographic symmetry. This oscillation will in turn displace the tip which is in intimate contact with the surface. The vertical (Fig. 1(c)) and lateral (Fig. 1(d)) components of displacement are measured with the SPM optical detector. The tip displacement signal is conditioned further using a lock-in amplifier, which amplifies only the components of the displacement signal corresponding to the driving frequency. Tip position is correlated with the output signal from the lock-in to generate piezoelectric amplitude and phase response maps.

The AFAM experimental set-up (Fig. 1(b)) includes a piezo-actuator positioned between the substrate and the microscope stage.¹¹ The actuator is set to oscillate at a constant amplitude and frequency during the entire scan. The amount of vertical displacement that is transferred to the tip via the substrate depends on local hardness. Therefore, AFAM images are maps of variations in the

substrate stiffness. As with PFM, the tip deflection signal is conditioned with a lock-in amplifier.

PFM, AFAM, and UFM measurements are implemented on a commercial SPM system (Veeco MultiMode NS-III) equipped with additional function generators and lock-in amplifiers (DS 345 and SRS 830, Stanford Research Instruments, Model 7280, Signal Recovery). For AFAM and UFM measurements, the samples were glued to the commercial PZT oscillator.¹² A custom-build sample holder was used to allow direct tip biasing and to avoid capacitive cross-talk in the SPM electronics. Measurements were performed using Pt and Au coated tips (NCSC-12 C, Micromasch, $l \approx 130 \mu\text{m}$, resonant frequency $\sim 150 \text{ kHz}$, spring constant $k \sim 4.5 \text{ N/m}$), which were found to provide optimal performance in PFM measurements. To maximize AFAM contrast, measurements were performed with softer tips (NCSC-36 C, Micromasch, $l \approx 130 \mu\text{m}$, resonant frequency $\sim 70 \text{ kHz}$, spring constant $k \sim 0.5 \text{ N/m}$). Lock-in amplifiers are used to determine the magnitude and phase of the cantilever response at the frequencies of modulation signals. Custom LabView software was used to emulate additional data acquisition channels and simultaneously acquire VPFM, LPFM, and AFAM data.

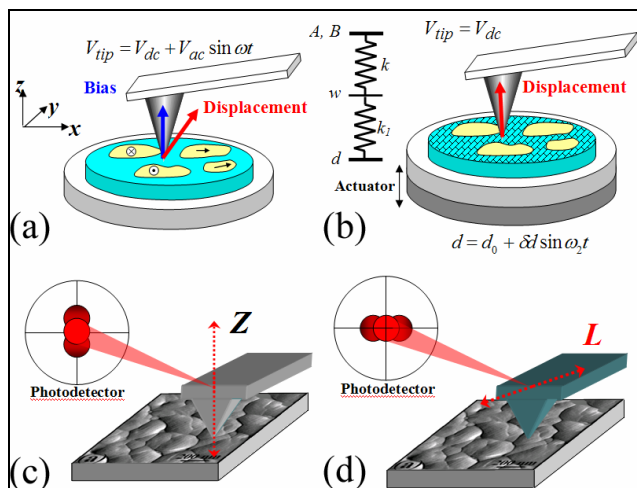


Figure 1: Experimental techniques. (a) In PFM, contrast originates from differences in mechanical response to an applied electric bias over the scanning region. (b) In AFAM, the amount of vertical displacement of the substrate transferred to the tip depends upon local substrate stiffness. (c) Vertical tip displacement detection. (d) Lateral tip deflection detection.

3 RESULTS

The high spatial resolution of SPM was used to study local elastic and piezoelectric properties in a broad range of inorganic materials.¹³ However, with a very few exceptions,¹⁴ the electromechanical properties of the calcified tissues were studied only on the macroscopic samples. Due to the complex hierarchical structure of most calcified tissues,¹⁵ macroscopic studies are associated with significant level of uncertainty, and not only the numerical

values of the piezoelectric constants, but also the symmetric of piezoelectric constant tensor is subject to controversy.

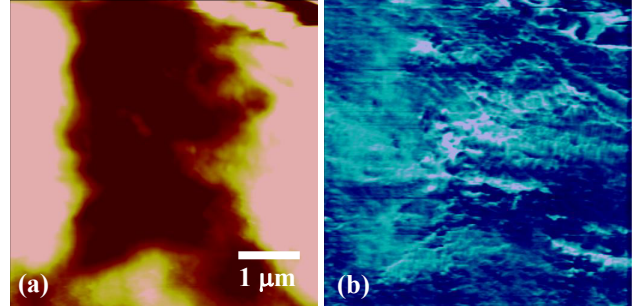


Figure 2: Topographic (a), and ultrasonic image of a deer antler. UFM reveals otherwise hidden nanoscale variations in mechanical and topographic properties.

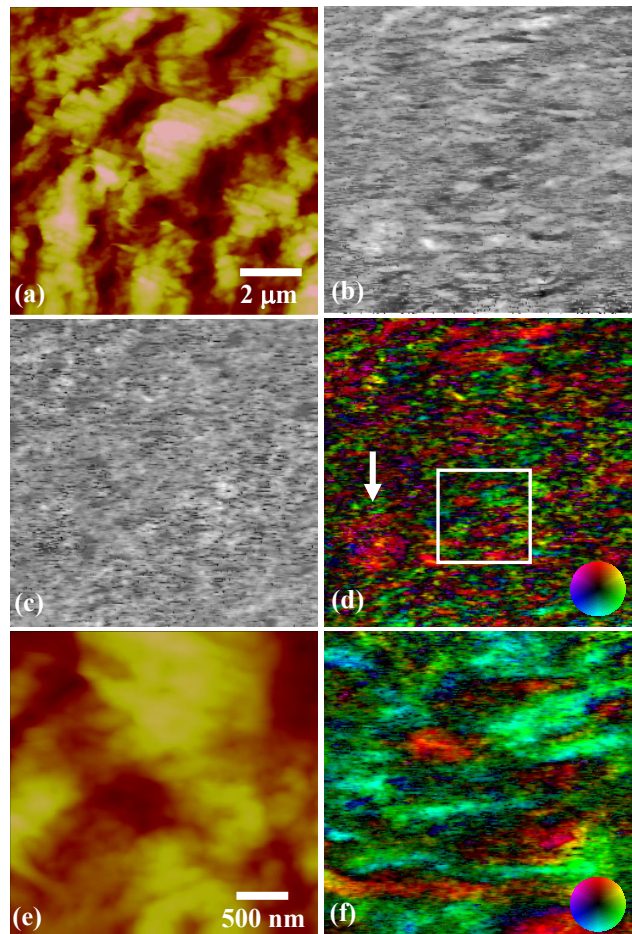


Figure 3: Surface topography (a), vertical (b) and lateral (c) PFM images of longitudinal cross-section of outer layer of deer antler. Note the presence of oriented keratin fibers on VPFM image. (d) Vector PFM images illustrates finer details of internal antler structure, including the presence of region with different keratin orientation. High resolution topography (e) and Vector PFM (f) images of the region marked by square in (d). The characteristic keratin fiber size in PFM image is $\sim 200 \text{ nm}$. Note that there is no correlation between PFM and topographic images, suggesting absence of cross-talk.

The use of local SPM techniques potentially allows electromechanical and elastic properties to be probed on a level of single building block of calcified tissues, such as individual hydroxyapatite (HAP) crystals and collagen fibrils in teeth and bones. We have used this approach to study local piezoelectricity in a broad range of tissues including teeth dentin and enamel, cartilage, bone, seashell, antler and butterfly wing. Here, we demonstrate the feasibility of this approach on an example of mapping local elastic and electromechanical properties of deer antler.

Shown in Fig. 2 is surface topography and Ultrasonic Force Microscopy (UFM) image of the perpendicular antler cross-section. The topography exhibits a number of features presumably related to the surface damage. Complementary UFM image illustrates local contrast variations across the image related to either topographic cross-talk, or intrinsic property variation in the material. Note that effective resolution in the UFM image is significantly higher than in topographic data, and has been shown to be ~ 5 nm, which is comparable with the tip-surface contact area for the used imaging conditions.

One of the limitations of acoustic techniques, such as AFAM and UFM, is the sensitivity to topographic cross-talk due to the changes in local surface geometry (slope and local radius of curvature) that influences the contact mechanics of the tip-surface junction. In addition, the signal in AFAM and UFM is strongly related to the tip shape and radius of curvature, necessitating the use of calibration standards with known properties for quantitative interpretation of these techniques. As opposed to it, electromechanical measurements by PFM are virtually insensitive to the tip geometry,¹⁶ resulting in significantly less sensitivity of the technique to topographic cross-talk thus providing direct pathway for quantitative electromechanical measurements on the nanoscale.

Figure 3 illustrates surface topography and piezoresponse images of longitudinal cross-section of the antler. Vertical PFM (Fig. 3b) clearly shows elongated features 2-3 μm long and 200-300 nm wide attributed to keratin fibrils, oriented along the antler axis. In comparison, lateral PFM (Fig. 3c) shows more randomized contrast due to the variations in the in-plane orientation of fibrils. Thus, VPFM and LPFM images show different patterns of piezoelectric domains, suggesting a complicated internal structure of tissue. To visualize electromechanical response data, we employ vector representation for PFM. The VPFM and LPFM images are normalized with respect to the maximum and minimum values of the signal amplitude so that the intensity changes between -1 and 1, i.e. $v_{pr}, l_{pr} \in (-1, 1)$. Using commercial software,¹⁷ these 2D vector data (v_{pr}, l_{pr}) is converted to the amplitude/angle pair, $A_{2D} = \text{Abs}(v_{pr} + i l_{pr})$, $\theta_{2D} = \text{Arg}(v_{pr} + i l_{pr})$. These data are plotted so that the color corresponds to the orientation, while color intensity corresponds to the magnitude, as shown in color wheel diagram. Note that unlike conventional SPM where pseudocolor images are

used for more vivid representation of scalar (height, current, etc) images, here the color is used to represent the local vector field orientation. The color encoded vector response map (Vector PFM), is shown in Fig. 3d. Note additional details on the microscopic texture visualized on the 2D vector PFM map, as indicated by arrow.

Shown in Fig. 3 e,f are enlarged scans, showing more clearly the topographic and piezoelectric properties of the surface, clearly visualizing the keratin fibril structure.

While calcified tissues, such as teeth, bones, and antlers, are robust enough to allow macroscopic assessment of mechanical and electrical properties, the majority of interesting biological materials are either too fragile or too small to be studied by conventional means. To evaluate the potential of SPM to probe local electro-mechanical and elastic properties in such systems, we have turned to assessing the nano-structural and nano-elastic properties of a butterfly wing¹⁸ - a system hardly amenable to previously available mechanical and piezoelectric measurement methods.

Shown in Fig. 4(a) is the butterfly *Vanessa virginiensis* (American Lady). The wing is covered with thousands of chitin scales. The top surfaces of the scales exhibit an intricate microstructure consisting of larger ridges extending longitudinally from one end of the scale to the other interconnected by a series of smaller crossribs (Fig. 4(b)).

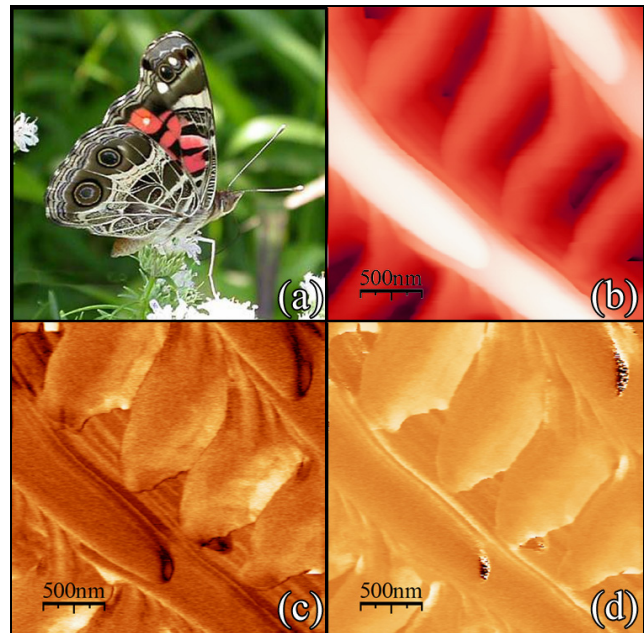


Figure 4: (a) Optical photograph of *Vanessa Virginiensis* (courtesy of Jeffrey Phippen, Duke University) and (b) AFM surface topography of the wing. (c) AFAM amplitude image (d) AFAM phase image. (b,c,d) were captured simultaneously. Note the difference in resolution between topographic and AFAM images.

This complex structure yields high stability in the butterfly wing, making it simultaneously lightweight and rigid.

While the structure of butterfly wing has been studied previously by AFM and SEM, very little is known of their elastic and mechanical properties and the relation of these properties to biological functionality.

Figure 4(c,d) shows the AFAM amplitude and phase data captured simultaneous to topographic mapping. Note the striking difference in the effective resolution between the two images – while no features smaller than 100 nm can be distinguished in the topographic image, the AFAM image shows details with sub-10 nm resolution. Significant variations in elastic contrast are seen within an individual ridge, suggesting an internal structural inhomogeneity at fundamental biological length scales. The unique mechanical properties of butterfly wing scales originate from its structure, which is a biological composite of rods of chitin embedded in a protein matrix. Accessing this kind of information about structure and functionality of complex biosystems at such fundamental length scales is critical to understanding the origins of macroscopic behavior, and this type of study is applicable to a wide range of biological systems, far beyond butterfly wings. Furthermore, this understanding can be applied to the engineering of better artificial materials.

SUMMARY

The explicit relationship between piezoelectric and mechanical properties and molecular orientation and biological functionality is a key to understanding biological systems. The SPM approach for simultaneous imaging of electromechanical and elastic properties provides a new tool to study these properties on length scales from tens of microns to the 10 nm level, i.e. on the length scale of the individual building blocks where the structural properties originate. The SPM method will undoubtedly play a crucial role in improving the understanding of the structure-property-functionality relationship, molecular orientation imaging, as well as in the development and testing of biologically inspired micromechanical devices, such as biomimetic wings.

ACKNOWLEDGEMENTS

Research performed in part as a Eugene P. Wigner Fellow and staff member at the Oak Ridge National Laboratory, managed by UT-Battelle, LLC, for the U.S. Department of Energy under Contract DE-AC05-00OR22725 (SVK). Support from ORNL SEED funding is acknowledged (ABP and SVK). AG acknowledges financial support of the National Science Foundation (Grant No. DMR02-35632).

-
- ³ L. Yasuda, On the piezoelectric activity of bone, *J. Jpn. Orthop. Surg. Soc.* **28**, 267-269 (1957).
 - ⁴ J.C. Anderson and C. Eriksson, Piezoelectric properties of dry and wet bone, *Nature* **227**, 491-492 (1970).
 - ⁵ A.A. Marino and B.D. Gross, Piezoelectricity in Cementum, Dentine, and Bone, *Archs. Oral Biol.* **34** (7), 507-509 (1989).
 - ⁶ E. Fukada, Piezoelectricity of Wood, *J. Phys. Jpn.* **10**, 149-154 (1955), V.A. Bazhenov, Piezoelectric properties of wood, Consultants Bureau, New York, 1961
 - ⁷ V.A. Bazhenov, Piezoelectric properties of wood, Consultants Bureau, New York, 1961
 - ⁸ E. Fukada, Piezoelectricity of Biopolymers, *Biorheology* **32** (6), 593-609 (1995)
 - ⁹ C.A.L. Bassett, Biological Significance of Piezoelectricity, *Calc. Tiss. Res.* **1**, 252-272 (1968)
 - ¹⁰ A.A. Marino and R.O. Becker, Piezoelectric Effect and Growth Control in Bone, *Nature* **228**, 473-474 (1970)
 - ¹¹ U. Rabe, M. Kopycinska, S. Hiserkorn, J. Munoz-Saldana, G.A. Schneider, and W. Arnold, *J. Phys.* **D 35**, 2621 (2002).
 - ¹² SD 0.394-0.000-0.040-502, Piezo Kinetics, Bellefonte, PA 16823, www.piezo-kinetics.com
 - ¹³ A. Gruverman, in *Encyclopedia of Nanoscience and Nanotechnology*, edited by H.S.Nalwa, Vol. 3, pp.359-375 (American Scientific Publishers, Los Angeles, 2004).
 - ¹⁴ C. Halperin, S. Mutchnik, A. Agronin, M. Molotskii, P. Urenski, M. Salai, and G. Rosenman, *NanoLetters* **4**, 1253 (2004).
 - ¹⁵ B. Ji and H. Gao, *J. Mech. Phys. Solids* **52**, 1963 (2004).
 - ¹⁶ S.V. Kalinin, E. Karapetian, and M. Kachanov, *Phys. Rev. B* **70**, 184101 (2004)
 - ¹⁷ *Mathematika 5.0*, Wolfram Research
 - ¹⁸ The macroscopic segment of butterfly wing was mounted on the SiO₂/Si wafer using silver print and further mounted on the piezoactuator

¹ E. Fukada and I. Yasuda, On the piezoelectric effect of bone, *J. Phys. Soc. Jpn.* **12**, 1158-1162 (1957).

² S. B. Lang, *Nature*, November 12, No 5063, p 704 (1966).